Science of the Total Environment 618 (2018) 819–828

Contents lists available at ScienceDirect

Science of the Total Environment

journal homepage: www.elsevier.com/locate/scitotenv

A multidimensional comparison between MODIS and VIIRS AOD in estimating ground-level $PM_{2.5}$ concentrations over a heavily polluted region in China

Fei Yao [a], Menglin Si [a], Weifeng Li [b,c,*], Jiansheng Wu [a,d,**]

[a] Key Laboratory for Urban Habitat Environmental Science and Technology, Shenzhen Graduate School, Peking University, Shenzhen 518055, PR China
[b] Department of Urban Planning and Design, The University of Hong Kong, Hong Kong, SAR, China
[c] Shenzhen Institute of Research and Innovation, The University of Hong Kong, Shenzhen 518075, PR China
[d] Key Laboratory for Earth Surface Processes, Ministry of Education, College of Urban and Environmental Sciences, Peking University, Beijing 100871, PR China

HIGHLIGHTS

- The capacity of MODIS and VIIRS AOD were compared in terms of estimating $PM_{2.5}$.
- The MODIS model explained 71% of the total $PM_{2.5}$ variations.
- The VIIRS model with high-quality AOD explained 76% of the total $PM_{2.5}$ variations.
- The VIIRS models are capable of capturing high $PM_{2.5}$ concentrations.
- The practice of using medium-quality VIIRS AOD is meaningful.

GRAPHICAL ABSTRACT

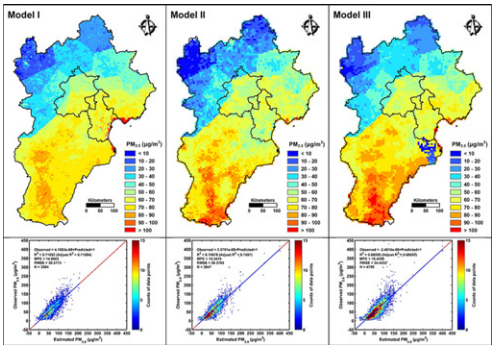

ARTICLE INFO

Article history:
Received 28 June 2017
Received in revised form 3 August 2017
Accepted 20 August 2017
Available online 11 November 2017

Editor: D. Barcelo

Keywords:
$PM_{2.5}$
Aerosol optical depth
MODIS
VIIRS
Fixed effects regression model
Beijing–Tianjin–Hebei

ABSTRACT

Satellite-derived aerosol optical depth (AOD) has been proven effective for estimating ground-level particles with an aerodynamic diameter <2.5 μm ($PM_{2.5}$) concentrations. Using a time fixed effects regression model, we compared the capacity of two AOD sources, Moderate Resolution Imaging Spectroradiometer (MODIS) and Visible Infrared Imaging Radiometer Suite (VIIRS), to estimate ground-level $PM_{2.5}$ concentrations over a heavily polluted region in China. Regarding high-quality AOD data, the results show that the VIIRS model performs better than the MODIS model with respect to all model accuracy evaluation indexes (e.g., the coefficient of determination, R^2, of the VIIRS and MODIS models are 0.76 and 0.71 during model fitting and 0.72 and 0.66 in cross validation, respectively), the potential for capturing high $PM_{2.5}$ concentrations, and the precision of annual and seasonal $PM_{2.5}$ estimates. However, the spatiotemporal coverage of the high-quality VIIRS AOD is inferior to that of the MODIS AOD. We attempted to include medium-quality VIIRS AOD data to eliminate this, while exploring its influence on the performance of the VIIRS model. The results show that it improves the spatiotemporal coverage of the VIIRS AOD dramatically especially in winter, although a decline in model accuracy occurred. Compared to the MODIS model, the VIIRS model with both high-quality and medium-quality AOD data performs comparably or even better with respect to some model accuracy evaluation indexes (e.g., the model overfitting degree of the VIIRS and MODIS models are 7.46% and 5.82%, respectively), the potential for capturing high $PM_{2.5}$ concentrations, and the precision of annual and seasonal $PM_{2.5}$ estimates. Nevertheless, the VIIRS models

* Correspondence to: W. Li, Department of Urban Planning and Design, The University of Hong Kong, Hong Kong, SAR, China.
** Correspondence to: J. Wu, Key Laboratory for Urban Habitat Environmental Science and Technology, Shenzhen Graduate School, Peking University, Shenzhen 518055, PR China.
E-mail addresses: wfli@hku.hk (W. Li), wujs@pkusz.edu.cn (J. Wu).

http://dx.doi.org/10.1016/j.scitotenv.2017.08.209

did not perform as well as the MODIS model in summer. This study reveals the advantages and disadvantages of the MODIS and VIIRS AOD in simulating ground-level $PM_{2.5}$ concentrations, promoting research on satellite-based $PM_{2.5}$ estimates.

1. Introduction

Numerous epidemiological studies have indicated that long-term exposure to particles with an aerodynamic diameter <2.5 μm ($PM_{2.5}$) is associated with various adverse health outcomes (Dominici et al., 2006; Pope et al., 2002; Pope and Dockery, 2006). With rapid urbanization and industrialization, China has become one of the worst regions with respect to fine particle pollution worldwide (Boys et al., 2014; van Donkelaar et al., 2015; van Donkelaar et al., 2016; van Donkelaar et al., 2010). Consequently, national $PM_{2.5}$-related deaths from stroke, ischemic heart disease, lung cancer, etc. have increased dramatically in the past decades (Liu et al., 2016; Wu et al., 2017).

Both epidemiological studies and environmental management efforts benefit from the estimation of spatially fine $PM_{2.5}$ concentrations with high accuracy, resolution, and spatiotemporal coverage. In contrast to limited, costly ground monitoring sites with an uneven spatial coverage in China, satellite remote sensing technology has the potential to achieve such estimations due to its high resolution and spatiotemporal coverage. It is a new and effective tool that has been developed rapidly in recent years (Hoff and Christopher, 2009).

Aerosol optical depth (AOD) is the most commonly used remote sensing parameter in satellite-based $PM_{2.5}$ estimation models, which is defined as the integral of the light extinction caused by aerosol optical absorption and scattering in an atmospheric column and has been proven to correlate with ground-level $PM_{2.5}$ concentrations (Engel-Cox et al., 2004; Hu et al., 2014; Wang and Christopher, 2003). A series of AOD products derived from satellite sensors have been adopted to estimate ground-level $PM_{2.5}$ concentrations. These include AOD products from the Moderate Resolution Imaging Spectroradiometer (MODIS) (Hu et al., 2013; Lee et al., 2011; Ma et al., 2016a; Ma et al., 2016b; Song et al., 2014), Multiangle Imaging SpectroRadiometer (MISR) (Liu et al., 2007; Liu et al., 2005; You et al., 2015), Visible Infrared Imaging Radiometer Suite (VIIRS) (Schliep et al., 2015; Wu et al., 2016), Geostationary Operational Environmental Satellite (GOES) (Liu et al., 2009), and Geostationary Ocean Color Imager (GOCI) (Xu et al., 2015).

Among the above-mentioned AOD products, MODIS AOD has been applied mostly due to its long time series of archived data (Chu et al., 2016). However, MODIS is already working beyond its expected operation period and is expected to cease transmitting data in the future. The VIIRS was designed and launched to address this. As a next-generation polar-orbiting operational environmental sensor with the capability for global aerosol observations, VIIRS aerosol retrieval is expected continue the decade-long successful aerosol retrieval of MODIS for scientific research and applications (Liu et al., 2014; Meng et al., 2015). Although some studies have shown that AOD products from the MODIS and VIIRS are both suitable for estimating ground-level $PM_{2.5}$ concentrations, few studies have compared their capacities. Such comparative studies are important for providing meaningful indications on the respective strengths of MODIS and VIIRS AOD, as well as offering helpful suggestions for improving the new VIIRS.

Therefore, the objective of this study is to compare the capacity of the MODIS and VIIRS AOD in estimating ground-level $PM_{2.5}$ concentrations over a heavily polluted region in China. To this end, we collected 3-km MODIS AOD and 6-km VIIRS AOD from the MODIS Collection 6 (C6) and the VIIRS Environmental Data Record (EDR), respectively. Subsequently, we established several separate satellite-based statistical $PM_{2.5}$ estimation models, one MODIS model and two VIIRS models, using MODIS and VIIRS AOD, respectively, as the main predicator, as well as several auxiliary variables. Next, we compared the capacities of the MODIS and VIIRS models from a multidimensional perspective. Finally, we determined whether the MODIS and VIIRS AOD differ significantly with respect to estimating ground-level $PM_{2.5}$ concentrations over a heavily polluted region in China and offered constructive suggestions on future applications of satellite-derived AOD.

2. Data and methods

2.1. Study area

We used the Beijing-Tianjin-Hebei region as the study area. It is located in Northern China, and includes the entire Beijing municipality, Tianjin municipality, and Hebei province. Due to the long history of industrial development and urban expansion, this region is heavily polluted and faces a greater health burden than other regions in China (Liu et al., 2016). From April 2014 to April 2015, half of the ten cities most affected by haze in China were located in this region, with a maximum annual $PM_{2.5}$ concentration of 118.08 μg/m^3 in Baoding, Hebei (Zhang and Cao, 2015). As the capital area in China, the fine particulate pollution in this region has attracted increasing attention from scholars, the government, and inhabitants. A total of 104 $PM_{2.5}$ monitors and 25 weather stations are distributed throughout this region (Fig. 1). The southeastern area is characterized by a lower terrain and concentration of main human activities.

2.2. Data collection

Ground-level $PM_{2.5}$ data were downloaded from the official website of the China Environmental Monitoring Center (CEMC) and Beijing Municipal Environmental Monitoring Center (BJMEMC). The data were measured using the tapered element oscillating microbalance method (TEOM) or the beta-attenuation method, which are automatic online monitoring methods stipulated by the new ambient air quality standards, and were processed using data quality calibration and control (HJ618-2011, 2011). The temporal resolution of the ground-level $PM_{2.5}$ measurements was 1 h; we used the daily average as the dependent variable.

The MODIS is an important sensor installed on the Terra and Aqua satellites (Remer et al., 2005) of the Earth Observing System (EOS) operated by the National Aeronautics and Space Administration (NASA). The MODIS AOD includes two types of AOD algorithms, the dark target (DT) and deep blue (DB) AOD algorithms. In the newest C6 collection, the MODIS team firstly released 3-km DT AOD products (Remer et al., 2013). We obtained the 3-km MODIS AOD data from the Terra and Aqua satellites from the Level-1 and Atmospheric Archive & Distribution System (LAADS) operated by NASA (code: MOD04_3K, MYD04_3K). The VIIRS is a key sensor onboard the Suomi National Polar-orbiting Partnership (Suomi-NPP) Satellite. It provides two types of AOD products, the intermediate product (IP) AOD and the EDR AOD, with spatial resolutions of 750 m and 6 km (Jackson et al., 2013), respectively. Both can be applied and explored when estimating ground-level $PM_{2.5}$ concentrations. In this study, we mainly aimed to compare the capacities of the 3-km MODIS AOD and 6-km VIIRS AOD to estimate ground-level $PM_{2.5}$ concentrations. Therefore, we collected the EDR AOD (code: VIIRS_EDR) from the Comprehensive Large Array-data Stewardship System (CLASS) operated by the National Oceanic and Atmospheric Administration (NOAA).

The AOD is the total integral of the light extinction caused by aerosol optical absorption and scattering in an atmospheric column. Its

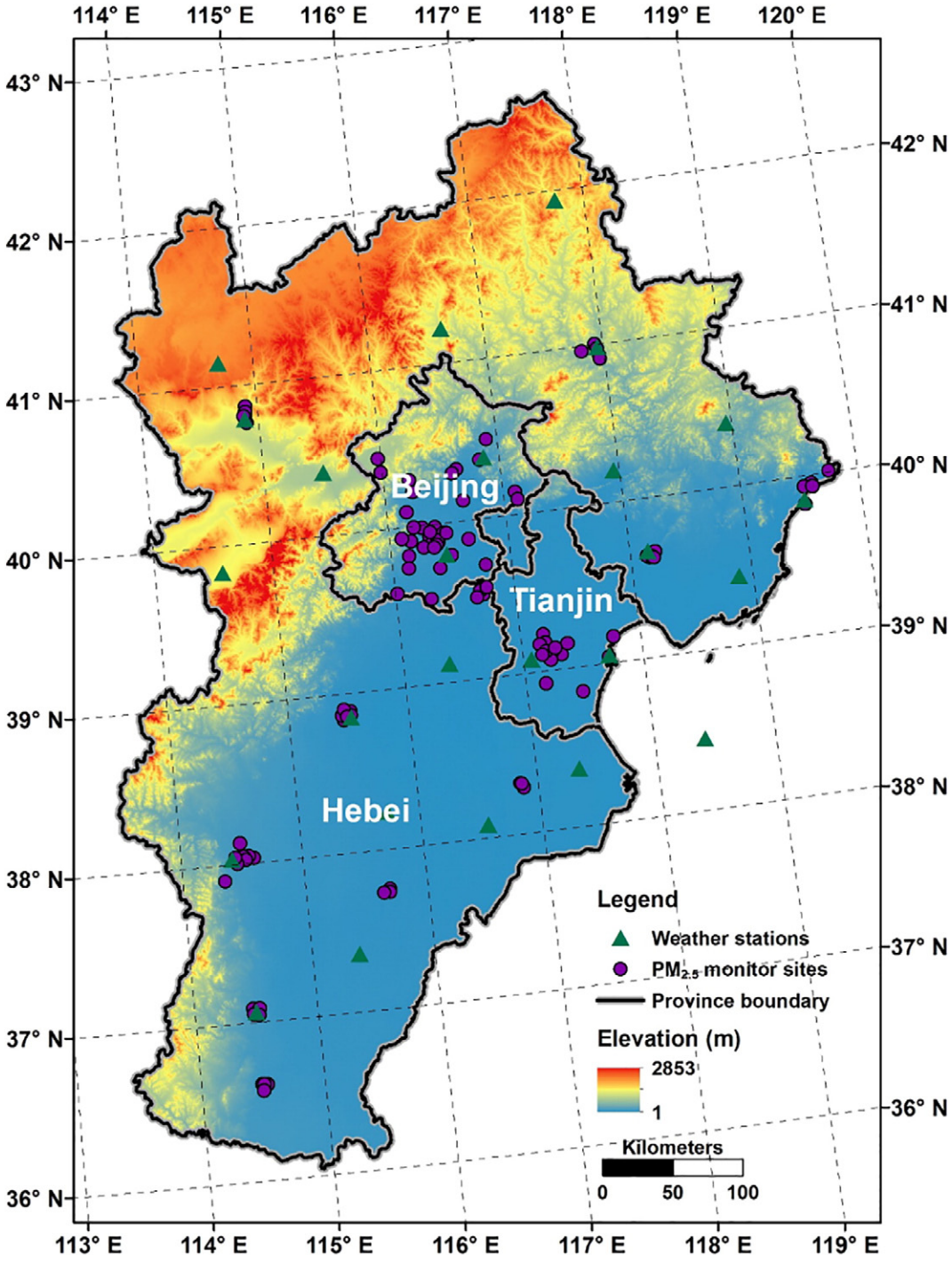

Fig. 1. Study area.

correlation with ground-level $PM_{2.5}$ concentration is affected by the vertical profile of the AOD. Studies have shown that most particles are uniformly distributed in the lower troposphere with intensive mixing (Clarke et al., 1996; Sheridan and Ogren, 1999). Thus, the planet boundary layer height (PBLH) can be used as a proxy in the model accounting for the vertical profile of the AOD and is negatively correlated with $PM_{2.5}$ (Liu et al., 2005). Aerosols increase due to moisture absorption, which changes its distribution and optical properties (Malm et al., 2000), influencing the $PM_{2.5}$–AOD relationship. In this study, the PBLH data and the average relative humidity data of the lower tropospheric nine layers at 1000 hPa, 975 hPa, 950 hPa, 925 hPa, 900 hPa, 875 hPa, 850 hPa, 825 hPa, and 800 hPa altitudes (RH_PBL) from the MERRA model reanalysis were incorporated into the model as assistant variables. Both PBLH (code: tavg1_2d_flx_Nx) and RH_PBL (code: inst3_3d_asm_Cp) data were downloaded from the Goddard Earth Sciences Data and Information Services Center (GES DISC) (Rienecker et al., 2011) with spatial resolutions of 0.5° × 0.5° and 1.25° × 1.25°, respectively. We used the average values during the satellite overpass time to adjust the model. Limited by the temporal resolution, the PBLH and RH_PBL data were averaged from 12:30 to 14:30 and 12:00 to 15:00 local time, respectively.

Surface meteorological conditions either increase or decrease the ground-level $PM_{2.5}$ concentrations and consequently influence the $PM_{2.5}$–AOD relationship. In this study, we obtained the temperature

(TEMP), surface relative humidity (SRH), precipitation (PRCP), wind direction during maximum wind speed (WD), and wind speed (WS) data from the China Meteorological Data Sharing System. Data with a 1-day temporal resolution from 25 weather stations in Beijing-Tianjin-Hebei were included (Fig. 1). We used the daily averages for TEMP and SRH, and daily summation for PRCP. Based on the WD and WS, we derived four wind vectors using the strategy described by (Wu et al., 2016): east wind speed (EWS), south wind speed (SWS), west wind speed (WWS), and north wind speed (NWS). The surface meteorological data were all incorporated into the model to adjust the $PM_{2.5}$–AOD relationship.

In addition, plant foliage decreases ground-level $PM_{2.5}$ concentrations by absorbing particles on the plant leaf surfaces or in leaf wax (Nowak et al., 2006; Pugh et al., 2012). Thus, we added the normalized difference vegetation index (NDVI) to the model, which is a proxy for surface vegetation coverage and its change, to further adjust the $PM_{2.5}$–AOD relationship. Moreover, low vegetation areas generally represent highly developed areas; therefore, a negative correlation between NDVI and $PM_{2.5}$ can be derived. NDVI data with temporal and spatial resolutions of 16 days and 250 m, respectively, were downloaded from LAADS (code: MOD13Q1).

Finally, several other atmospheric pollutants, such as NO_2, can be used as a proxy for anthropogenic emissions (Zhang and Cao, 2015) and influence the $PM_{2.5}$–AOD relationship. Following the method used by (Wu et al., 2016), we added the previous day's NO_2 concentrations to the model to obtain good model performance. NO_2 data from the ozone monitoring instrument (OMI) sensor were downloaded from the Tropospheric Emission Monitoring Internet Service (TEMIS) (Boersma et al., 2011). The spatial resolution of the OMI NO_2 data was $0.25^\circ \times 0.25^\circ$.

All of the above-mentioned data were collected from January 1 to December 31, 2014. The URLs (Uniform Resource Locators) for these data are listed in the supplementary material (Table S1).

2.3. Quality assurance of AOD

In addition to the AOD products, the MODIS and VIIRS teams also release the corresponding quality assurance (QA) data. The interpretation of MODIS and VIIRS QA data is shown in Table 1. In this study, we used QA = 2, 3 MODIS AOD and QA = 2, 3 VIIRS AOD data to avoid the potential negative effects of AOD deviations.

We combined the two types of satellite MODIS AOD data before building the MODIS model, because the MODIS sensor is installed on both the Terra and Aqua satellites. We used the MODIS AOD on the Terra and Aqua satellites of each day and ordinary least square (OLS) regression method to fit the equation for the Aqua and Terra MODIS AOD. To ensure the accuracy, only days with >30 Terra and Aqua MODIS AOD data pairs with correlation coefficients no <0.5 were processed. We obtained the fitted Aqua MODIS AOD by applying the equation to the Terra MODIS AOD pixels. The fitted Aqua MODIS AOD was used to complement the missing Aqua MODIS AOD to form the combined Aqua MODIS AOD. We used the combined Aqua MODIS AOD to build the MODIS model (Model I) because the satellite overpass time of Aqua (1:30 pm) coincides with that of the Suomi-NPP satellite. The OLS fusion method has been proven effective in previous studies (Ma et al., 2014; Puttaswamy et al., 2014) and eliminates the systematic differences of various satellite-derived AOD values.

Differing from the MODIS, the VIIRS provides a medium-quality AOD data product. Since we have no prior knowledge of its predictive power for ground-level $PM_{2.5}$ concentrations, we used QA = 3 and QA = 2, 3 AOD data to build the two VIIRS models (Model II, Model III), respectively. A comparison between them could reveal the tradeoff between their spatiotemporal coverage and predictive power for ground-level $PM_{2.5}$ concentrations. Comparing them with Model I could reveal the capacity differences between MODIS and VIIRS AOD in estimating ground-level $PM_{2.5}$ concentrations, which is the objective of this study.

Table 1
Quality assurance flags of MODIS and VIIRS AOD.

MODIS		VIIRS	
Flag	Quality	Flag	Quality
0	Bad or no confidence	0	Not produced
1	Marginal	1	Low
2	Good	2	Medium
3	Very good	3	High

2.4. Data integration

The data employed in this study comprise different data types, coordinate systems, and spatiotemporal resolutions. Before establishing the models, we projected all data into the Albers equal-area conic coordinate system. Then, we matched all independent variables to $PM_{2.5}$ monitors using the nearest neighbor method. With respect to the mapping data, we first created 3-km grids and 6-km grids in the Beijing–Tianjin–Hebei region according to the spatial resolutions of the MODIS and VIIRS AOD. Then, we used the nearest neighbor method again to match all independent variables to the grids.

2.5. Model fitting and validation

Modeling and mapping datasets were obtained after the data integration; the datasets were spatial unbalanced panel data, meaning that each data record is related to a specific day and specific site, but the number of data records for a specific day or a specific site varies greatly. We omitted the data for days with less than two records to enable cross-validation. There are various statistical methods for spatial unbalanced panel data. In this study, we employed the time fixed effects regression model because of the computational savings, easy operation, and comparable model performance in contrast to linear mixed effects models (Wu et al., 2016). The model structure is as follows:

$$\begin{aligned} PM_{2.5,st} = {} & \lambda_t + \beta_{AOD} AOD_{st} + \beta_{PBLH} PBLH_{st} + \beta_{RH\_PBL} RH\_PBL_{st} \\ & + \beta_{TEMP} TEMP_{st} + \beta_{SRH} SRH_{st} + \beta_{PRCP} PRCP_{st} + \beta_{EWS} EWS_{st} \\ & + \beta_{SWS} SWS_{st} + \beta_{WWS} WWS_{st} + \beta_{NWS} NWS_{st} + \beta_{NDVI} NDVI_{st} \\ & + \beta_{NO_2\_Lag} NO_2\_Lag_{st} + \varepsilon_{st} \end{aligned} \quad (1)$$

where $PM_{2.5,st}$, AOD_{st}, $PBLH_{st}$, RH_PBL_{st}, $TEMP_{st}$, SRH_{st}, $PRCP_{st}$, EWS_{st}, SWS_{st}, WWS_{st}, NWS_{st}, and $NDVI_{st}$ are the ground-level $PM_{2.5}$ concentrations, AOD, PBLH, RH_PBL, TEMP, SRH, PRCP, EWS, WWS, SWS, and NWS at site s during day t; $NO_2\_Lag_{st}$ is the NO_2 concentration at site s during day $t-1$; and β_{AOD}, β_{PBLH}, β_{RH_PBLH}, β_{TEMP}, β_{SRH}, β_{PRCP}, β_{EWS}, β_{SWS}, β_{WWS}, β_{NWS}, β_{NDVI}, and $\beta_{NO_2\_Lag}$ are the coefficients of AOD, PBLH, RH_PBLH, TEMP, SRH, PRCP, EWS, SWS, WWS, NWS, NDVI, and NO_2_Lag. λ_t is the intercept during day t, reflecting the daily variation of the $PM_{2.5}$–AOD relationship.

By applying the model dataset to Eq. (1), we obtained the coefficients and intercepts of the model, from which we estimated the $PM_{2.5}$ concentrations for both monitors and non-monitors. We regressed the $PM_{2.5}$ estimations to observations at monitors and calculated several statistical parameters, including the coefficient of determination (R^2), mean predication error (MPE), and root mean square error (RMSE), to assess the model's fitting capability. To assess the generalizability of the model, we conducted a ten-fold cross-validation. We randomly split the dataset into ten subsets and completed ten rounds of model fitting and prediction. In each round, we used nine subsets to fit the model; the tenth subset was used for the prediction. We obtained another data pair between the $PM_{2.5}$ estimations and observations after the ten rounds were completed. Similarly, we fitted a regression equation and used the same statistics to assess the generalizability of the model.

2.6. Ground-level $PM_{2.5}$ mapping and evaluation

We estimated the ground-level $PM_{2.5}$ concentrations of each day by combining the fitting model with the mapping dataset. We further obtained the annual and seasonal ground-level $PM_{2.5}$ concentrations by averaging the daily estimates of the whole year or four seasons, respectively. For annual and seasonal estimations, we assessed their deviations from the observations.

3. Results

3.1. Descriptive analysis

Table S2 summarizes the descriptive statistics of the modeling dataset. In general, most variables of Models I, II, and III have a similar distribution. Three main differences should be noted. First, the maximum value and standard deviation of the ground-level $PM_{2.5}$ concentrations of Models II and III are larger, indicating that the VIIRS matches larger and wider ground-level $PM_{2.5}$ concentrations. Second, the AOD ranges of MODIS (0–4) and VIIRS (0–2) differ, indicating potential differences when estimating ground-level $PM_{2.5}$ concentrations. Third, Model I is larger than Model II, benefiting from the simultaneous installation of MODIS on Terra and Aqua satellites. However, Model I is smaller than Model III, indicating that including medium-quality VIIRS AOD can obtain more regression data pairs, exceeding the advantage of the simultaneous installation of MODIS on the Terra and Aqua satellites.

3.2. Spatiotemporal coverage of AOD

Fig. 2 illustrates the spatiotemporal coverage of the MODIS and VIIRS AOD. Each raster value represents the proportion of days for which AOD was derived. Table 2 shows the corresponding averages over the whole region. Regarding high-quality AOD retrievals, the MODIS performs better than the VIIRS during the whole year, spring, summer, and autumn, which is mainly due to the simultaneous installation of MODIS on two satellites. However, the VIIRS performs much better than the MODIS in winter, even though it is only associated with one satellite. After including the medium-quality AOD, the spatiotemporal coverage of the VIIRS AOD outperforms the MODIS AOD during the whole year and most seasons, especially winter. Because fine particulate pollution in China is worse in winter (Ma et al., 2014; Zhang and Cao, 2015), the VIIRS has the potential to capture high $PM_{2.5}$ concentrations.

3.3. Model fitting

Table 3 summarizes the coefficients and intercepts of the MODIS and VIIRS models. Most variables have the same signs and are significant at the $\alpha = 0.05$ level. PBLH and NDVI are not significant in all models. However, the signs of these two variables in the VIIRS models are in accord with prior knowledge (Liu et al., 2005; Wu et al., 2016), while those in the MODIS model are not. Moreover, the p values of these two variables in the VIIRS models are much smaller than those in the MODIS model. Regarding the four wind vectors, the MODIS model has three non-significant variables, while the VIIRS models have one or two insignificant variables with smaller p values. Although the NO_2_lag variable is not significant in Model II, its p value is only 0.079. In general, the VIIRS models perform better than the MODIS model based on the variable significance test. However, including the medium-quality VIIRS AOD results in a slight decrease in the performance of the VIIRS model.

3.4. Model validation

Fig. 3 illustrates the model fitting and generalizability of Models I, II, and III. Fig. 4 shows their benchmark models, namely, the non-AOD model with all other variables. The following three results indicate that Model II is the best among the three models. First, the model fitting and cross-validation of Model II have the highest R^2, lowest MPE, and lowest RMSE values. Second, the slope of Model II is nearest to one and the intercept of Model II is nearest to zero. Third, Model II can derive high $PM_{2.5}$ concentrations (>300 μg/m^3). A comparison of Models II and

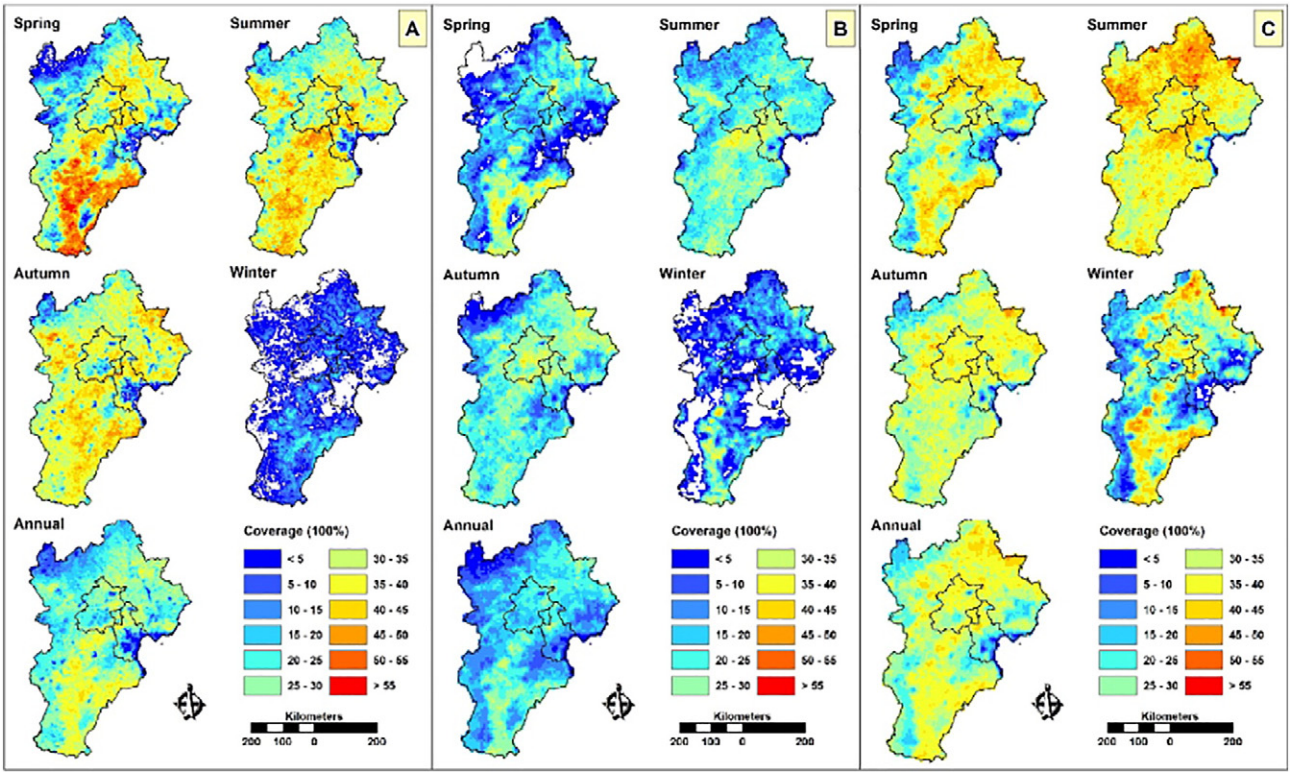

Fig. 2. Spatiotemporal coverage of AOD (A: MODIS, B: VIIRS QA = 3, C: VIIRS QA = 2, 3).

Table 2
Coverage averages over the whole region.

AOD parameter	Spring coverage (%)	Summer coverage (%)	Autumn coverage (%)	Winter coverage (%)	Annual coverage (%)
MODIS	29.16	33.06	32.89	4.78	25.06
VIIRS (QA = 3)	15.54	22.30	21.61	8.51	17.02
VIIRS (QA = 2, 3)	30.23	38.06	31.77	24.88	31.27

III shows that including medium-quality VIIRS AOD decreases the performance of the VIIRS model. The R^2 during model fitting and cross validation decreases by 9.71% and 10.03%, respectively. Meanwhile, the RMSE during model fitting and cross validation increases by 16.57% and 14.86%, respectively. Nevertheless, the annual coverage average over the whole region dramatically increases by 45.57% according to Table 2. A comparison of Models I and Model III shows that Model I has a higher R^2 (3.5%, 1.79% higher during model fitting and cross validation), lower MPE, and lower RMSE (15.99%, 13.91% lower during model fitting and cross validation). However, the slopes and intercepts of Model III are nearer to one and zero, respectively. The annual coverage average over the whole region of the QA = 2, 3 VIIRS AOD is higher than that of the MODIS AOD by 19.86% according to Table 2. Moreover, Model III inherits the capability of Model II to derive $PM_{2.5}$ concentrations higher than 300 μg/m^3, which is not characterized by Model I. Therefore, including medium-quality VIIRS AOD offers meaningful improvements. Although it decreases the model's performance with respect to R^2, MPE, and RMSE, it increases the coverage of AOD dramatically, retains the potential of the original model to derive high $PM_{2.5}$ concentrations, and yields a comparable or even better model performance compared to the MODIS model. The comparison of Models I, II, and III and their benchmark models shows that AOD can simultaneously improve model performance and decrease the degree of model overfitting. Simply using the decreased percentage of R^2 from the model fitting to cross validation, we calculated the model overfitting degrees for Models I, II, and III and their benchmark models (Table 4). As shown in Table 4, employing AOD decreases the model overfitting degree by 5.16%, 10.05%, and 21.37% for Models I, II, and III, providing additional evidence that the VIIRS models outperform the MODIS model.

3.5. Ground-level $PM_{2.5}$ mapping and evaluation

Fig. 5 illustrates the annual and seasonal $PM_{2.5}$ estimates from Models I, II, and III. The $PM_{2.5}$ estimates from all models present similar seasonal-spatial patterns. Specifically, the ground-level $PM_{2.5}$ concentrations are high in winter, low in summer, and moderate in spring and autumn. Spatially, the ground-level $PM_{2.5}$ concentrations are high in the southeastern area and low in the northwestern area, in agreement with the distribution of terrain and human activities described in Section 2.1. However, there are still some differences in the $PM_{2.5}$ estimates from the MODIS and VIIRS models. For example, the spatiotemporal coverage of the $PM_{2.5}$ estimates occurs in winter, i.e., Model III outperforms Models I and II dramatically, underlining the importance of including medium-quality VIIRS AOD. Another difference can be observed in the value size of the $PM_{2.5}$ estimates. Except in summer, the VIIRS models provide $PM_{2.5}$ estimates with slightly larger value sizes in the southeastern area. To analyze this difference, we plotted the annual and seasonal residuals at the monitors, as shown in Fig. 6, and their corresponding boxplots, as shown in Fig. 7. Figs. 6 and 7 indicate that satellite-based annual or seasonal $PM_{2.5}$ estimates underestimate the actual levels during the whole year and in most seasons. Thus, the second difference provides evidence for the finding that the VIIRS models outperform the MODIS model. Finally, we should note that the MODIS model outperforms the two VIIRS models in summer with respect to lower residuals, as shown in Figs. 6 and 7.

4. Discussion

In this study, we established three separate remote satellite-based statistical $PM_{2.5}$ estimation models for Beijing–Tianjin–Hebei using the MODIS and VIIRS AOD, respectively, and various assistant variables. The multidimensional comparison revealed that the VIIRS models outperformed the MODIS model. The practice of including medium-quality VIIRS AOD was determined to be viable, and improved the spatiotemporal coverage of the VIIRS AOD dramatically despite decreasing the model accuracy to some extent. To our knowledge, this is one of the first empirical studies to examine the differences between the remote sensing retrievals of ground-level $PM_{2.5}$ concentrations from MODIS and VIIRS over a heavily polluted region in China.

4.1. Comparison of MODIS and VIIRS models

The VIIRS AOD has a better capability to retrieve ground-level $PM_{2.5}$ concentrations based on the following evidence. First, Model II performed the best during the model fitting and cross-validation with respect to the significant variable numbers, signs and *p* values of variables, and model accuracy (e.g., R^2, MPE, and RMSE). Second, the seasonal estimates of ground-level $PM_{2.5}$ from Model III had the highest

Table 3
Coefficients and intercepts for models I, II, and III.

Variable	Model I				Model II				Model III			
	β	p	5%	95%	β	p	5%	95%	β	p	5%	95%
AOD (Unitless)	26.513	0.000	24.014	29.011	23.880	0.000	20.800	26.959	26.591	0.000	23.756	29.427
TEMP (0.1 °C)	0.460	0.000	0.407	0.514	0.542	0.000	0.484	0.600	0.495	0.000	0.448	0.542
SRH (%)	0.798	0.000	0.687	0.910	1.077	0.000	0.951	1.203	1.218	0.000	1.112	1.324
PRCP (0.1 mm)	−0.035	0.003	−0.058	−0.012	−0.054	0.011	−0.096	−0.012	−0.044	0.004	−0.073	−0.014
PBLH (m)	0.001	0.602	−0.002	0.003	−0.002	0.110	−0.005	0.001	−0.001	0.498	−0.003	0.002
RH_PBLH (Unitless)	−23.688	0.000	−34.584	−12.792	−26.147	0.000	−39.593	−12.701	−27.001	0.000	−38.857	−15.145
NDVI (Unitless)	1.812	0.521	−3.727	7.350	−5.756	0.059	−11.725	0.214	−5.206	0.081	−11.051	0.639
NO_2_Lag (10^{15} molec/cm^2)	0.376	0.000	0.251	0.501	0.127	0.079	−0.015	0.269	0.512	0.000	0.395	0.629
WWS (0.1 m/s)	0.060	0.308	−0.055	0.175	−0.079	0.270	−0.221	0.062	0.070	0.212	−0.040	0.180
NWS (0.1 m/s)	−0.122	0.057	−0.248	0.004	−0.342	0.000	−0.494	−0.191	−0.208	0.000	−0.321	−0.095
EWS (0.1 m/s)	−0.044	0.510	−0.177	0.088	−0.291	0.001	−0.465	−0.117	−0.048	0.492	−0.186	0.090
SWS (0.1 m/s)	−0.316	0.000	−0.432	−0.200	−0.242	0.002	−0.395	−0.089	−0.134	0.048	−0.267	−0.001

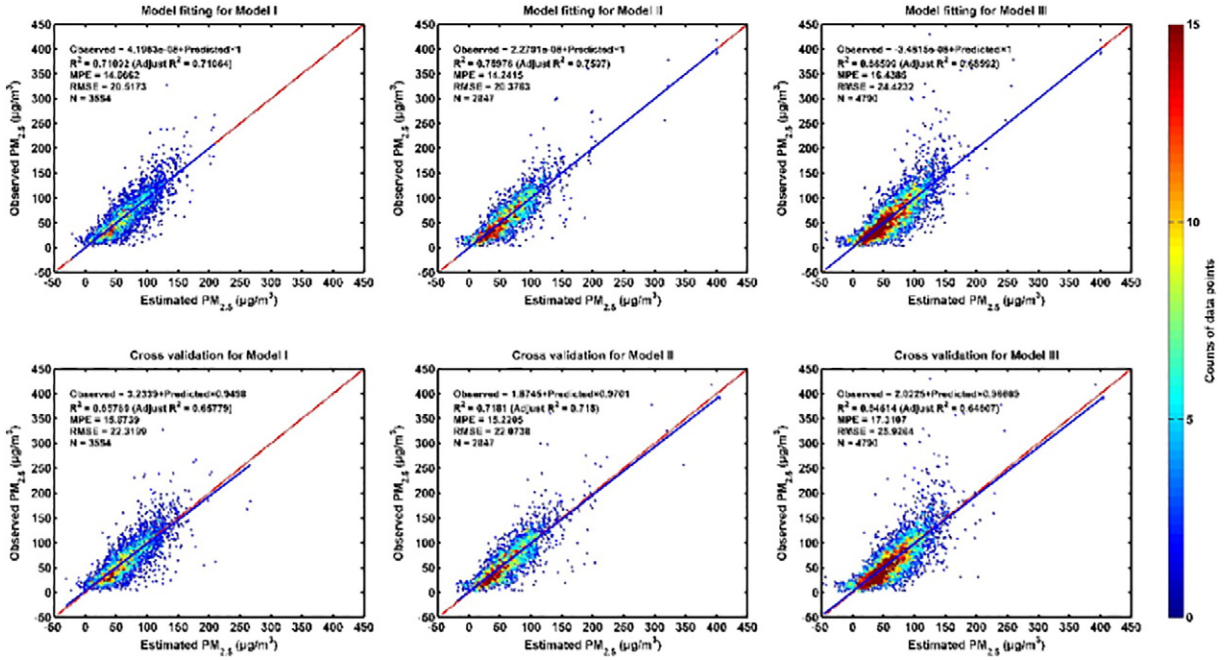

Fig. 3. Model validation for Models I, II, and III.

spatiotemporal coverage, especially in winter. Third, both Models II and III could retrieve high $PM_{2.5}$ concentrations and have lower model overfitting degrees, while Model I did not. Finally, except in summer, the annual and seasonal ground-level $PM_{2.5}$ concentrations from Models II and III were closer to the actual levels. We attribute the advantages of the VIIRS AOD to the following points. First and foremost, the MODIS and VIIRS have different service durations. The MODIS was installed on Terra and Aqua in December 1999, and May 2002, respectively, with a prospective life of 6 years (Remer et al., 2005). The VIIRS was installed on Suomi-NPP in October 2011, with a prospective life of 7 years (Jackson et al., 2013). The MODIS onboard Terra and Aqua have undergone different rates of instrumental degradation in the past decade (Chen et al., 2014; Lyapustin et al., 2014), causing a decline in the data quality over time. To eliminate instrumental degradation, the MODIS team has continuously improved the AOD retrieving algorithm. The MODIS 3-km AOD used in this study was obtained from the latest MODIS C6 (Remer et al., 2013). However, it is difficult to completely eliminate instrumental degradation. In a recent study, the VIIRS, GOCI,

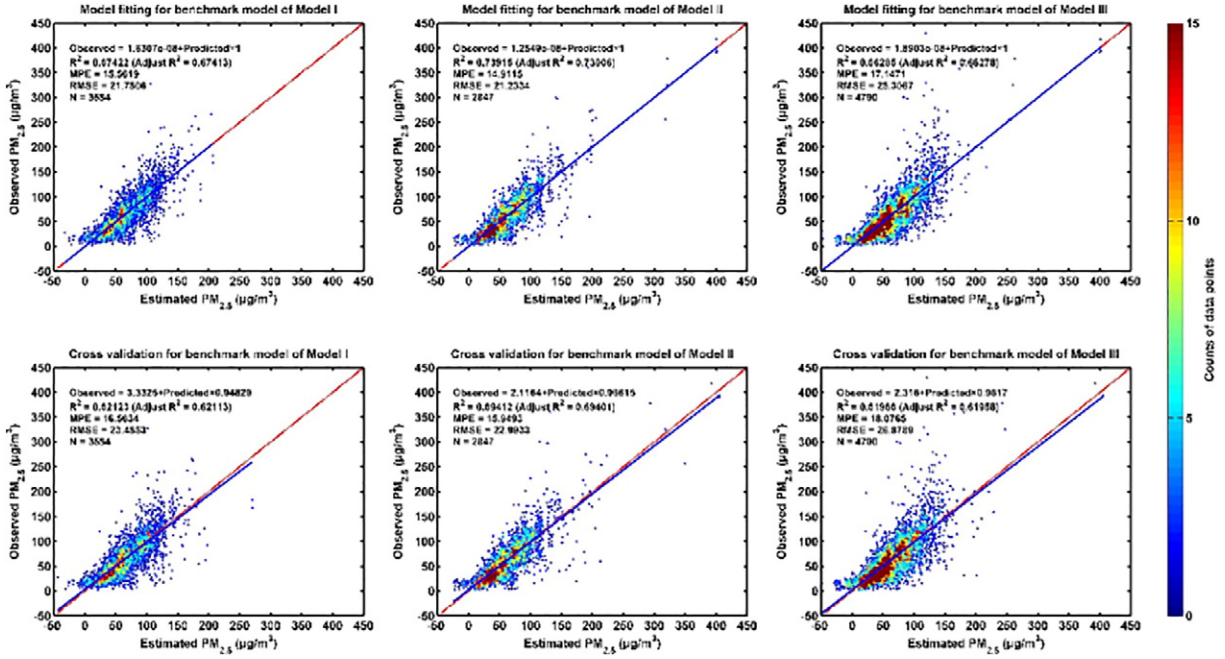

Fig. 4. Model validation for the benchmark models of Models I, II, and III.

Table 4
Model overfitting degree for models I, II, and III and their benchmark models.

Model	Model overfitting degree % (full model)	Model overfitting degree % (benchmark model)
I	7.46	7.86
II	5.49	6.10
III	5.82	7.40

and MODIS C6 AOD were compared with that from ground AOD observations over East Asia. The VIIRS EDR and GOCI products provided the most accurate AOD retrievals, while the VIIRS IP and MODIS C6 3-km products had a positive bias (Xiao et al., 2016). Second, the VIIRS was designed as an expansion and improvement of the MODIS and Advanced Very High Resolution Radiometer (AVHRR), achieving substantial improvements in the quality of the radiation measurement, spectral measurement range, and spatial resolution (Schueler et al., 2002). Thus, such data is likely to have a greater potential for monitoring ground-level air quality. Other than the ability of capturing high $PM_{2.5}$ concentrations revealed in this study, the VIIRS day/night band has been proven to have the potential to monitor nighttime surface $PM_{2.5}$ (Wang et al., 2016).

While the better performance of the VIIRS AOD in estimating ground-level $PM_{2.5}$ concentrations is encouraging, its deficiencies should not be ignored. The annual and seasonal residual analysis reveals that the MODIS model performs better in summer with lower deviations. After replotting Fig. 3 using only the data pairs from summer, we found that MODIS model performed much better than the two VIIRS models with respect to higher R^2 values during both model fitting and cross validation (0.6737, 0.65302, 0.61948 during model fitting and 0.63631, 0.61587, 0.57759 during cross validation for Models I, II, and III), slopes and intercepts nearer to one and zero (slope: 1.0035, 0.94127, 0.89978 during model fitting and 0.969, 0.9101, 0.86246 during cross validation for Models I, II, and III; intercept: −0.21332, 3.0261, 5.304 during model fitting and 1.8949, 4.676, 7.2484 during cross validation for Models I, II, and III), and a lower model overfitting degree (5.55%, 5.68%, 6.76% for Models I, II, and III). Therefore, caution should be taken when using the VIIRS AOD to estimate ground-level $PM_{2.5}$ concentrations, at least over this study area in summer.

4.2. Assessment of including medium-quality VIIRS AOD

Differing from the MODIS, the VIIRS provides a medium-quality AOD data product. Since we have no prior knowledge of this kind of data, we explored its influence on the performance of the VIIRS model. The results show that this practice provides meaningful results, and the benefit of the AOD spatiotemporal coverage improvement significantly outweighs the model accuracy decline. With respect to the variable significance test, model overfitting degree, and annual and seasonal deviations, the VIIRS model with medium-quality AOD performed comparably or even better than the MODIS model. To alleviate the influence on VIIRS model accuracy introduced by the medium-quality AOD data, we added a QA dummy variable into Model III to establish a QA-controlled time fixed effects regression model. However, it only improved the R^2 by 0.04% during model fitting and offered no improvement in cross validation. Further studies could consider using ground observation AOD data, such as ground AOD observations from the Aerosol Robotic Network (AERONET), and handheld sunphotometers to correct the medium-quality VIIRS AOD data before the model construction, which may improve the model accuracy to a larger degree.

4.3. Limitations and prospects of this study

The time fixed effects regression model employed in this study provides an individual intercept for each day, reflecting the temporal heterogeneity of the $PM_{2.5}$-AOD relationship. However, daily intercepts cannot be determined for days without $PM_{2.5}$-AOD matchups. Consequently, daily $PM_{2.5}$ estimations on such days cannot be estimated, even if there are abundant data available at non-monitoring sites, which is one of the limitations of this study. Similar to the time fixed effects regression model, the linear mixed effects regression model (LME)

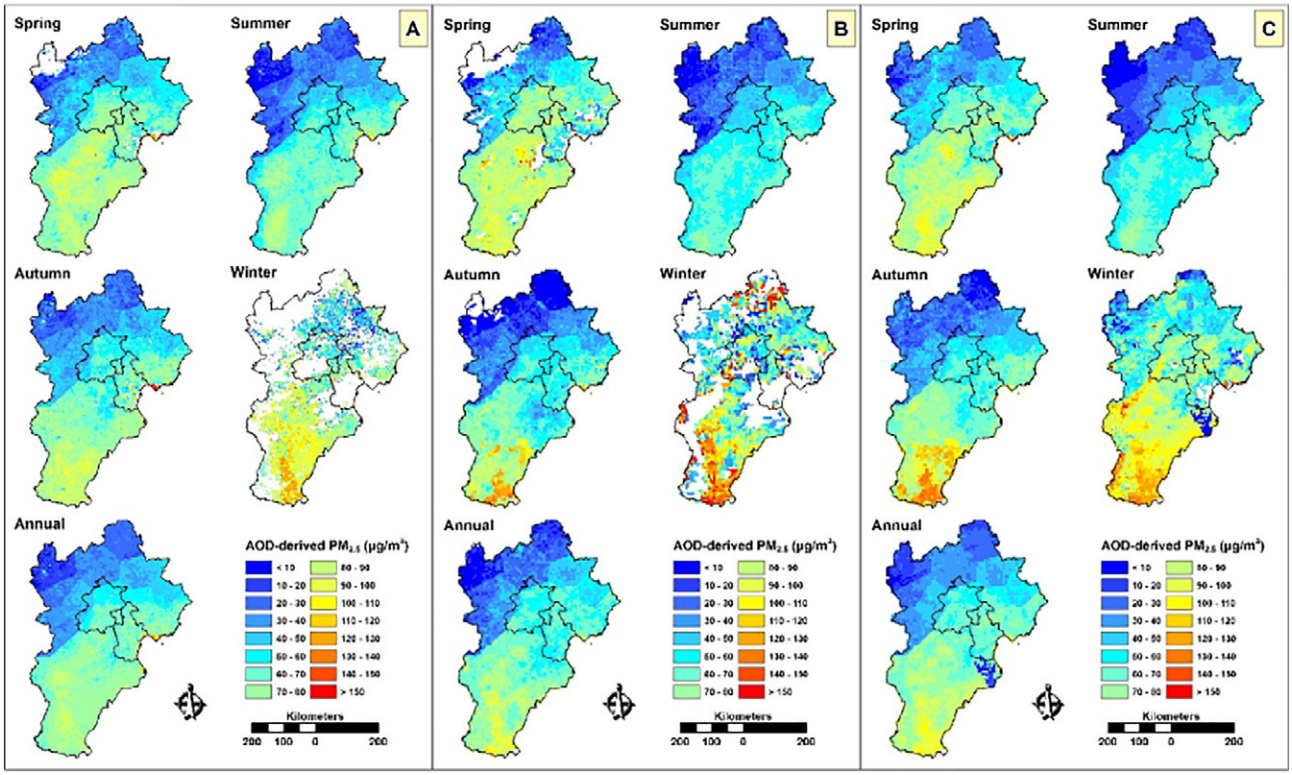

Fig. 5. Ground-level $PM_{2.5}$ estimates from MODIS and VIIRS models (A: Model I, B: Model II, C: Model III).

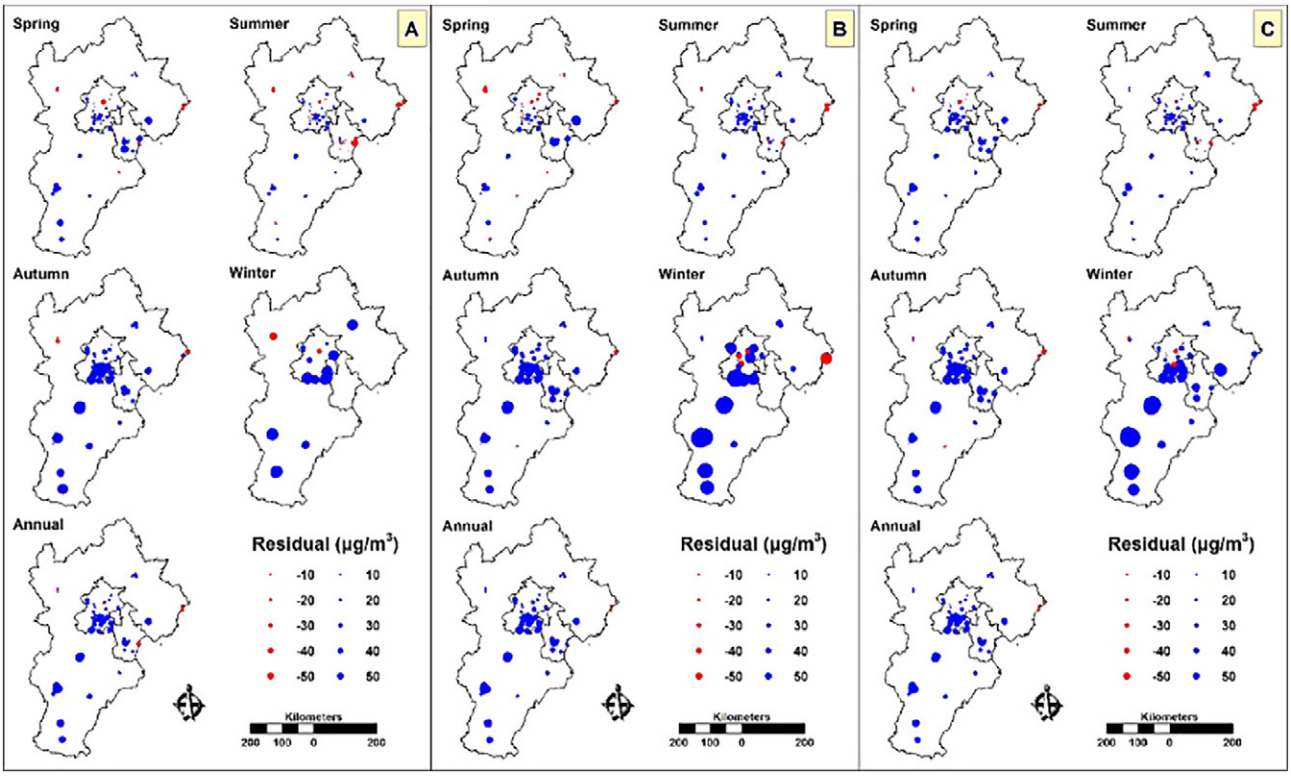

Fig. 6. The residuals at each monitoring site.

has the same problem. A nested linear mixed effects regression model was developed for the Yangtze River Delta in a recent study to abate this issue, and good performance was reported (Ma et al., 2016b). Therefore, we could develop a similar nested time fixed effects regression model in the future to address this limitation. Compared to previous studies, which also use 3-km MODIS AOD and 6-km VIIRS AOD data to estimate ground-level $PM_{2.5}$ concentrations in China, the model accuracy of our study is as good as those using the LME model (Ma et al., 2016b) but inferior to those using the geographical weighted regression model (You et al., 2016) or two-stage spatiotemporal statistical model (Wu et al., 2016). Ignoring the spatial variation of the $PM_{2.5}$-AOD relationship is the underlying reason for the slightly lower model accuracy. However, the main objective of this study was to compare the capacity of the 3-km MODIS AOD and 6-km VIIRS AOD in estimating ground-level $PM_{2.5}$ concentrations. Moreover, the spatial variations of the estimated $PM_{2.5}$ can be explained by the spatial variation of the AOD data. Therefore, the model accuracy might not be to blame. Nevertheless, in future studies, both the temporal and spatial heterogeneity of the $PM_{2.5}$-AOD relationship should be considered when the main goal is to estimate spatially fine ground $PM_{2.5}$ concentrations with high accuracy using satellite-based models to avoid large biases, especially in large areas.

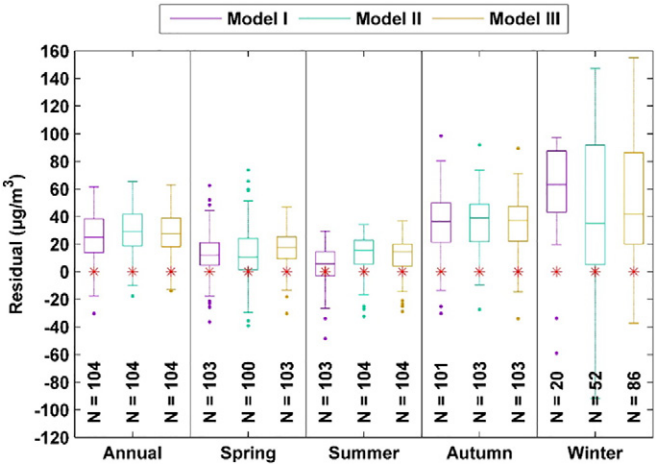

Fig. 7. Boxplot of the residuals.

5. Conclusions

The main contribution of this study is that we have revealed the differences between the 3-km MODIS AOD and 6-km VIIRS AOD for estimating ground-level $PM_{2.5}$ concentrations, despite several limitations. From the perspective of the accuracy and capacity of the model, the VIIRS models outperform the MODIS model, especially when only high-quality AOD data are used. From the perspective of annual and seasonal $PM_{2.5}$ estimates, the VIIRS models provide more estimates closer to actual levels, especially in winter. Nevertheless, the VIIRS models do not perform as well as the MODIS model in summer, which should be considered in future research. The findings of this study indicate that, for epidemiological or urban studies that require precise $PM_{2.5}$ estimates, the VIIRS AOD is better, whereas for regional source or transport studies, the MODIS AOD could still have a role due to its wider spatiotemporal coverage, especially in summer.

Acknowledgements

This study was financially supported by the National Natural Science Foundation of China (No. 41330747 and No. 41471370). We thank anonymous reviewers and the editor for their constructive comments.

Appendix A. Supplementary data

Supplementary data to this article can be found online at http://dx.doi.org/10.1016/j.scitotenv.2017.08.209.

References

Boersma, K.F., Eskes, H.J., Dirksen, R.J., van der A RJ, Veefkind JP, Stammes P, et al., 2011. An improved tropospheric NO_2 column retrieval algorithm for the ozone monitoring instrument. Atmos. Meas. Tech. 4, 1905–1928.

Boys, B.L., Martin, R.V., van Donkelaar, A., MacDonell, R.J., Hsu, N.C., Cooper, M.J., et al., 2014. Fifteen-year global time series of satellite-derived fine particulate matter. Environ. Sci. Technol. 48, 11109–11118.

Chen, H., Li, Q., Wang, Z., Mao, H., Zhou, C., Zhang, L., et al., 2014. Study on monitoring surface $PM_{2.5}$ concentrations in Jing-Jin-Ji regions using MODIS data. J. Meteorol. Environ. 30, 27–37.

Chu Y, Liu Y, Li X, Liu Z, Lu H, Lu Y, et al. A Review on predicting ground PM2.5 concentration using satellite aerosol optical depth. Atmosphere 2016; 7.

Clarke, A.D., Porter, J.N., Valero, F.P.J., Pilewskie, P., 1996. Vertical profiles, aerosol microphysics, and optical closure during the Atlantic stratocumulus transition experiment: measured and modeled column optical properties. J. Geophys. Res. Atmos. 101, 4443–4453.

Dominici, F., Peng, R.D., Bell, M.L., Pham, L., McDermott, A., Zeger, S.L., et al., 2006. Fine particulate air pollution and hospital admission for cardiovascular and respiratory diseases. Jama J. Am. Med. Assoc. 295, 1127–1134.

Engel-Cox, J.A., Holloman, C.H., Coutant, B.W., Hoff, R.M., 2004. Qualitative and quantitative evaluation of MODIS satellite sensor data for regional and urban scale air quality. Atmos. Environ. 38, 2495–2509.

HJ618-2011, 2011. Determination of Atmospheric Articles PM10 and PM2.5 in Ambient Air by Gravimetric Method. http://english.mep.gov.cn/standards_reports/.

Hoff, R.M., Christopher, S.A., 2009. Remote sensing of particulate pollution from space: have we reached the promised land? J. Air Waste Manage. Assoc. 59, 645–675.

Hu, X.F., Waller, L.A., Al-Hamdan, M.Z., Crosson, W.L., Estes, M.G., Estes, S.M., et al., 2013. Estimating ground-level PM2.5 concentrations in the southeastern US using geographically weighted regression. Environ. Res. 121, 1–10.

Hu, X.F., Waller, L.A., Lyapustin, A., Wang, Y.J., Al-Hamdan, M.Z., Crosson, W.L., et al., 2014. Estimating ground-level PM2.5 concentrations in the Southeastern United States using MAIAC AOD retrievals and a two-stage model. Remote Sens. Environ. 140, 220–232.

Jackson, J.M., Liu, H.Q., Laszlo, I., Kondragunta, S., Remer, L.A., Huang, J.F., et al., 2013. Suomi-NPP VIIRS aerosol algorithms and data products. J. Geophys. Res.-Atmos. 118, 12673–12689.

Lee, H.J., Liu, Y., Coull, B.A., Schwartz, J., Koutrakis, P., 2011. A novel calibration approach of MODIS AOD data to predict PM2.5 concentrations. Atmos. Chem. Phys. 11, 7991–8002.

Liu, Y., Sarnat, J.A., Kilaru, A., Jacob, D.J., Koutrakis, P., 2005. Estimating ground-level PM2.5 in the eastern United States using satellite remote sensing. Environ. Sci. Technol. 39, 3269–3278.

Liu, Y., Franklin, M., Kahn, R., Koutrakis, P., 2007. Using aerosol optical thickness to predict ground-level PM2.5 concentrations in the St. Louis area: a comparison between MISR and MODIS. Remote Sens. Environ. 107, 33–44.

Liu, Y., Paciorek, C.J., Koutrakis, P., 2009. Estimating regional spatial and temporal variability of PM(2.5) concentrations using satellite data, meteorology, and land use information. Environ. Health Perspect. 117, 886–892.

Liu, H., Huang, J., Jackson, I.L.A.M., 2014. Preliminary evaluation of S-NPP VIIRS aerosol optical thickness. J. Geophys. Res. Atmos. 119, 3942–3962.

Liu, M., Huang, Y., Ma, Z., Jin, Z., Liu, X., Wang, H., et al., 2016. Spatial and temporal trends in the mortality burden of air pollution in China: 2004–2012. Environ. Int. 98, 75.

Lyapustin, A., Wang, Y., Xiong, X., Meister, G., Platnick, S., Levy, R., et al., 2014. Scientific impact of MODIS C5 calibration degradation and C6+ improvements. Atmos. Meas. Tech. 7, 4353–4365.

Ma, Z., Hu, X., Huang, L., Bi, J., Liu, Y., 2014. Estimating ground-level PM2. 5 in China using satellite remote sensing. Environ. Sci. Technol. 48, 7436–7444.

Ma, Z., Hu, X., Sayer, A.M., Levy, R., Zhang, Q., Xue, Y., et al., 2016a. Satellite-based spatiotemporal trends in PM2.5 concentrations: China, 2004–2013. Environ. Health Perspect. 124, 184–192.

Ma, Z.W., Liu, Y., Zhao, Q.Y., Liu, M.M., Zhou, Y.C., Bi, J., 2016b. Satellite-derived high resolution PM2.5 concentrations in Yangtze River Delta region of China using improved linear mixed effects model. Atmos. Environ. 133, 156–164.

Malm, W.C., Day, D.E., Kreidenweis, S.M., 2000. Light scattering characteristics of aerosols at ambient and as a function of relative humidity: part II - a comparison of measured scattering and aerosol concentrations using statistical models. J. Air Waste Manage. Assoc. 50, 701–709.

Meng, F., Cao, C., Shao, X., 2015. Spatio-temporal variability of Suomi-NPP VIIRS-derived aerosol optical thickness over China in 2013. Remote Sens. Environ. 163, 61–69.

Nowak, D.J., Crane, D.E., Stevens, J.C., 2006. Air pollution removal by urban trees and shrubs in the United States. Urban For. Urban Green. 4, 115–123.

Pope, C.A., Dockery, D.W., 2006. Health effects of fine particulate air pollution: lines that connect. J. Air Waste Manage. Assoc. 56, 709–742.

Pope, C.A., Burnett, R.T., Thun, M.J., Calle, E.E., Krewski, D., Ito, K., et al., 2002. Lung cancer, cardiopulmonary mortality, and long-term exposure to fine particulate air pollution. Jama J. Am. Med. Assoc. 287, 1132–1141.

Pugh, T.A.M., MacKenzie, A.R., Whyatt, J.D., Hewitt, C.N., 2012. Effectiveness of green infrastructure for improvement of air quality in urban street canyons. Environ. Sci. Technol. 46, 7692–7699.

Puttaswamy, S.J., Nguyen, H.M., Braverman, A., Hu, X.F., Liu, Y., 2014. Statistical data fusion of multi-sensor AOD over the continental United States. Geocarto Int. 29, 48–64.

Remer, L.A., Kaufman, Y.J., Tanre, D., Mattoo, S., Chu, D.A., Martins, J.V., et al., 2005. The MODIS aerosol algorithm, products, and validation. J. Atmos. Sci. 62, 947–973.

Remer, L.A., Mattoo, S., Levy, R.C., Munchak, L.A., 2013. MODIS 3 km aerosol product: algorithm and global perspective. Atmos. Meas. Tech. 6, 1829–1844.

Rienecker, M.M., Suarez, M.J., Gelaro, R., Todling, R., Bacmeister, J., Liu, E., et al., 2011. MERRA: NASA's modern-era retrospective analysis for research and applications. J. Clim. 24, 3624–3648.

Schliep, E., Gelfand, A., Holland, D., 2015. Autoregressive spatially varying coefficients model for predicting daily PM 2.5 using VIIRS satellite AOT. Adv. Stat. Climatol. Meteorol. Oceanogr. 1, 59.

Schueler, C.F., Clement, J.E., Ardanuy, P.E., Welsch, C., DeLuccia, F., Swenson, H., 2002. NPOESS VIIRS sensor design overview. International symposium on optical science and technology. Int. Soc. Opt. Photon. 11–23.

Sheridan, P.J., Ogren, J.A., 1999. Observations of the vertical and regional variability of aerosol optical properties over central and eastern North America. J. Geophys. Res. Atmos. 104, 16793–16805.

Song W, Jia H, Huang J, Zhang Y. A satellite-based geographically weighted regression model for regional PM2.5 estimation over the Pearl River Delta region in China. Remote Sens. Environ. 2014; 154: 1–7.

van Donkelaar, A., Martin, R.V., Brauer, M., Kahn, R., Levy, R., Verduzco, C., et al., 2010. Global estimates of ambient fine particulate matter concentrations from satellite-based aerosol optical depth: development and application. Environ. Health Perspect. 118, 847–855.

van Donkelaar, A., Martin, R.V., Brauer, M., Boys, B.L., 2015. Use of satellite observations for long-term exposure assessment of global concentrations of fine particulate matter. Environ. Health Perspect. 123, 135–143.

van Donkelaar, A., Martin, R.V., Brauer, M., Hsu, N.C., Kahn, R.A., Levy, R.C., et al., 2016. Global estimates of fine particulate matter using a combined geophysical-statistical method with information from satellites, models, and monitors. Environ. Sci. Technol. 50, 3762–3772.

Wang, J., Christopher, S.A., 2003. Intercomparison between satellite-derived aerosol optical thickness and PM2. 5 mass: implications for air quality studies. Geophys. Res. Lett. 30.

Wang, J., Aegerter, C., Xu, X., Szykman, J.J., 2016. Potential application of VIIRS day/night band for monitoring nighttime surface PM2.5 air quality from space. Atmos. Environ. 124, 55–63.

Wu J, Yao F, Li W, Si M. VIIRS-based remote sensing estimation of ground-level PM 2.5 concentrations in Beijing–Tianjin–Hebei: a spatiotemporal statistical model. Remote Sens. Environ. 2016; 184: 316–328.

Wu, J., Zhu, J., Li, W., Xu, D., Liu, J., 2017. Estimation of the PM2.5 health effects in China during 2000–2011. Environ. Sci. Pollut. Res. Int. 24, 1–13.

Xiao, Q., Zhang, H., Choi, M., Li, S., Kondragunta, S., Kim, J., et al., 2016. Evaluation of VIIRS, GOCI, and MODIS collection 6 AOD retrievals against ground sunphotometer observations over East Asia. Atmos. Chem. Phys. 16, 1255–1269.

Xu, J., Martin, R., Kim, J., Choi, M., Zhang, Q., Geng, G., et al., 2015. Estimating ground-level PM2.5 in China using aerosol optical depth determined from the GOCI satellite instrument. Atmos. Chem. Phys. 15, 13133–13144.

You, W., Zang, Z., Pan, X., Zhang, L., Chen, D., 2015. Estimating PM2.5 in Xi'an, China using aerosol optical depth: a comparison between the MODIS and MISR retrieval models. Sci. Total Environ. 505, 1156–1165.

You W, Zang Z, Zhang L, Li Y, Pan X, Wang W. National-scale estimates of ground-level PM2.5 concentration in China using geographically weighted regression based on 3 km Resolution MODIS AOD. Remote Sens. 2016; 8: 184.

Zhang, Y.L., Cao, F., 2015. Fine particulate matter (PM2.5) in China at a city level. Sci. Rep. 5, 14884.